Microwave-Assisted Extraction of Cellulose from Waste Olive Wood Powder Using Deep Eutectic Solvents

Mohammad Mahbubul Alam
University of Salento
Antonio Greco
University of Salento
Carola Esposito Corcione
University of Salento
Alfonso Jiménez
alfjimenez@ua.es
University of Alicante
María Carmen Garrigós
University of Alicante

Research Article

Keywords: microwave-assisted extraction, deep eutectic solvents, olive powder, cellulose, characterization

Posted Date: August 17th, 2024

DOI: https://doi.org/10.21203/rs.3.rs-4720873/v1

Additional Declarations: No competing interests reported.

Abstract

Microwave-assisted extraction (MAE) is a very effective and sustainable method for extracting cellulose from lignocellulosic materials due to the substantial reduction in the process time and amounts of solvents required for each process. Deep eutectic solvents (DES) are used for cellulose extraction due to their environmental friendliness and high extraction yields. This work explores the possibility to use microwave-synthesized DES to extract cellulose from olive wood powder (OWP) waste. The conventional process (CP) requires the use of high amounts of chemicals and long times for quantitative extractions. Three techniques for the cellulose extraction were compared: a standard procedure by Technical Association of the Pulp and Paper Industry (TAPPI), CP, and MAE utilizing DES to evaluate the effectiveness of these techniques. Results showed that the TAPPI method yielded 55.0 wt% cellulose, whereas the CP method yielded 50.6 wt% cellulose. The optimum conditions for MAE using choline chloride-lactic acid (ChCl:LA, 1:4) and choline chloride-citric acid (ChCl:CA:H_2O, 1:1:6) were found to be 20-min irradiation time at 130 ºC to obtain cellulose yields of 47.8 wt% and 45.6 wt%, respectively, showing that both DES were effective for cellulose extraction from OWP. The comparison between all procedures showed that MAE required shorter times and smaller quantities of chemicals, making it an eco-friendlier option. The extracted cellulose was characterized by thermogravimetric analysis (TGA), Fourier transform infrared spectroscopy (FTIR), X-ray diffraction (XRD), and Scanning electron microscopy (SEM). Results suggested that MAE with DES is a promising approach, with prospective applications in the packaging, textiles, and paper industries.

Introduction

The bacterial plant pathogen “Xylella” caused significant mortality and inflicted substantial damage to olive trees in the Puglia region, in southern Italy. Therefore, it became necessary to identify appropriate uses for the leftover olive wood coming from damaged trees. Like other lignocellulosic biomasses, olive tree pruning (OTP) biomass contains cellulose, hemicelluloses, lignin, soluble compounds (extractives), and ash. The chemical composition of OTP biomass depends on tree age, soil type, and climate (Gullón et al. 2018). Due to their particular properties, these biomaterials have several uses (Romero-García et al. 2014). As well known, cellulose can be extracted and utilized for various purposes, including the development of biodegradable plastics, textiles, and paper (Esposito Corcione et al. 2020; Ferrari et al. 2022). However, conventional techniques for cellulose extraction usually require the use of toxic chemicals and high temperatures, which pollute the environment (Boli et al. 2022).

The recycling of biomass waste, such as wood waste and agricultural husks, is becoming very important to obtain biomaterials with advanced properties and applications (Mujtaba et al. 2023). Recent research has focused on recycling natural polymers including cellulose, lignin, collagen, gelatin, keratin, and chitin/chitosan from biomass wastes, such rice husk, peanut shells, corncobs, skin, and fish, shrimp, and crab bones, to produce biomaterials, packaging films, and bioactive compounds (Rachiero et al. 2022). There are various pre-treatment techniques for converting biomass using different solvents, such as alkalis, acids, ionic liquids, deep eutectic solvents (DES), combined with physical processes (milling and

refining), biological methods, and physicochemical methods (Galbe and Wallberg 2019). Alkali or acid-based procedures were the traditional pre-treatment options, but showed major drawbacks, such as high risk of equipment damage, expensive waste water treatment costs, or chemicals recovery (Rastogi and Shrivastava 2017). In the conventional cellulose extraction process, an alkaline treatment (NaOH/KOH) requires 4–6 hours followed by a bleaching process ($NaClO/NaOCl_2$) that takes 1–2 hours (Ndruru et al. 2019). In this way, hemicelluloses bound to cellulose are separated during bleaching and the outcome becomes whiter. After an alkaline process that completely breaks down lignin, acidified sodium chlorite ($NaClO_2$) is typically utilized as the most adequate bleaching agent (Leite et al. 2017; Ndruru et al. 2019).

Microwave assisted extraction (MAE) is an innovative and environmentally-friendly method that utilizes electromagnetic radiation to enhance the efficiency of material extraction to obtain cellulose in less than one hour by speeding up biomaterial separation and cellulose dewaxing (Haldar and Purkait 2021; Azlan et al. 2022). Due to its "green" character and highly efficient extraction, MAE has grown in importance during the past 15 years. Indeed, microwave radiation increases residual water evaporation from raw materials and weakens plant cell walls to promote internal diffusion, making MAE superior to conventional extraction methods (Khandanlou et al. 2016; Chadni et al. 2019; Haldar and Purkait 2021). MAE is affected by the solvent's capacity to penetrate plant materials permitting solubilization and diffusion of cellulose (Kłosowski et al. 2020). Additionally, since heating in MAE is selective and targeted, very little energy is lost to the environment. Moreover, microwave power has been explored as a potential pre-treatment method for improving the production of different lignocellulosic by-products (Khandanlou et al. 2016; Azlan et al. 2022). Despite a large initial expenditure, microwave equipment has lower operational costs than traditional heating techniques, even a short preparation time (Puligundla et al. 2016).

In recent years, there has been much interest in the use of greener solvents in chemical processes because they pose fewer risks to human health, safety, and the environment. DES can be used as environmentally-friendly solvents for cellulose extraction (Wang et al. 2020). The two primary constituents of DES are hydrogen bond acceptors (HBA) and hydrogen bond donors (HBD). Owing to their low cost, quaternary ammonium salts, such as choline chloride (ChCl), have been used frequently to prepare DES. HBA and HBD mixtures create a eutectic with a melting point substantially lower than that of each of their individual components (Mamilla et al. 2019; Kohli et al. 2020; Alam et al. 2024). As green solvents for biomass pre-treatment and extraction, DES have emerged with a number of benefits, including ease of preparation, high purity, low toxicity, easy biodegradability, low melting temperatures, high thermal stability, low volatility, non-flammability, and high air stability (Isci et al. 2020; Kwon et al. 2021).

In this study, extensive experimental efforts were made to determine the best way to extract cellulose from waste OWP, considering the extraction yield of cellulose, crystallinity index, thermal behaviour, and morphological properties. This study also examined the use of MAE with various DES combinations as a sustainable and green method to get cellulose fractions to be further processed and used in different applications. The overall experimental MAE process was compared with the conventional cellulose

extraction method, and the advantages of less process steps, lower temperatures, and fewer extraction times were discussed.

Experimental

Materials and Methods

Olive tree (*Olea europaea*) branches were collected from a village farm near Lecce, Italy, and they were cut into small pieces at a local factory. A milling machine (Retsch Type ZM 100, Germany) was used to grind the wood. The particle size distribution of OWP was determined by a Microtrac MRB particle sizer (Germany).

All chemicals were of analytical grade and used without any prior purification, including ethanol (96.00%, PanReac AppliChem, Italy), toluene (≥ 99.70%, Honeywell/Fluka, Germany), sodium hydroxide pellets (≥ 98.00%, Honeywell/Fluka, Germany), sulfuric acid (95-97%, Honeywell/Fluka, Germany), acetic acid (≥ 99.80%, Honeywell/Fluka, Germany), Sodium Chlorite (80.00%, Honeywell/Fluka, Germany), choline chloride (≥ 98.00%, Sigma-Aldrich, China), lactic acid solution (≥ 85.00%, Sigma-Aldrich, USA), and anhydrous citric acid (PanReac AppliChem, Italy).

Composition measurement of OWP

The TAPPI Standards were used to evaluate the moisture (TAPPI T264 cm-97) and ash contents (TAPPI T211 om-02). The extractives content (TAPPI T204 cm-97), acid-insoluble lignin (TAPPI T222 om-02) Holocellulose, α-cellulose and hemicellulose contents were also determined (Wise et al. 1946; Rowell et al. 2005). The weight of α-cellulose was subtracted from the amount of holocellulose used to determine the hemicellulose content.

Conventional process (CP)

CP was applied to extract cellulose and lignin from the waste OWP. It was firstly treated with ethanol:toluene (1:2) mixture for 24 h at room temperature to eliminate extractives. After filtration, the extractive-free solid materials were dried for 24 h at 80 °C after being washed with distilled water. For the removal of hemicellulose and a greater portion of lignin, the extractive-free samples were treated with alkali solution (sodium hydroxide, 7%, w/v) at 90 °C for 90 min. Filtration with a microfiber filter (MFV3; filter lab) was performed on the alkaline-treated samples to collect the solids and separate the "black liquor". The solid materials were dried in an oven at 80 °C for 24 h after rinsing with distilled water until they reached a neutral pH. Sodium chlorite (5% w/v) was used to bleach the dry materials at 80 °C for 40 min. After filtration, samples were removed from the bleached liquor and washed thoroughly with hot and cold distilled water before drying for 24 h at 80 °C.

Synthesis of DES

DES were synthesized by using a Milestone FlexiWave™ microwave oven (Milestone Srl, Bergamo, Italy). Choline chloride (ChCl) was used as the HBA, while lactic acid (LA) and citric acid (CA) were utilized as HBD to separate cellulose biomass derived from waste OWP. DES were produced by combining ChCl and the respective HBDs in a precise proportion. This mixture was homogenized, and a clear solution was formed after microwave irradiation at 200 W for 4-8 min. The synthesis of ChCl and LA (in a 1:4 molar ratio), denoted as ChCl:LA (1:4), was achieved by applying 200 W of power for 4 min, resulting in the formation of a homogeneous and transparent liquid at 82 °C. DES based on ChCl and CA were produced at a 1:1:6 molar ratio, denoted as ChCl:CA:H_2O (1:1:6), using 200 W of power for 8 min. The reaction resulted in the formation of a homogeneous and transparent liquid at 96 °C. Figure 1 shows the scheme of a typical microwave set for the synthesis of DES.

Microwave Extraction Process

MAE was conducted in a microwave oven with a closed vessel setup, using DES generated as previously described. The quantity of ground waste OWP was set at 1.50 g within a sealed container, namely a round bottom flask, at temperatures 100 °C, 120 °C and 130 °C. The power used for extraction was 1600 W, and the processes lasted for 20 min in all extraction processes. Furthermore, vessels were kept inside the oven until they reached a lower temperature, suitable for safe handling. The extracted components were then filtered using a glass microfiber filter (MFV3; filter lab) and washed three times with distilled water to achieve a neutral pH in the filtrate. The specimen was then dehydrated at 60 °C for 24 h and thereafter kept at room temperature for the remaining steps. This approach simplifies the extraction of cellulose from OWP. The objective of this study was to maximize the production of cellulose from OWP by optimizing the microwave power, irradiation duration, and solvent proportion. Figure 2 shows the process flow diagram for cellulose extraction from waste OWP by using microwaves in a closed vessel with DES.

Characterization

Morphological analysis by scanning electron microscope (SEM)

The morphological structures of OWP, TAPPI process cellulose (TPC), and conventional process cellulose (CPC) samples were analyzed using a JEOL JSM-840 scanning electron microscope (Peabody, MA, USA) at an acceleration voltage of 5.00 kV. Prior to scanning, a SCD 004 Balzers sputter coater (Bal Tec. AG, Fürstentum, Lichtenstein) was used to coat the samples with a gold layer under vacuum. Morphological analyses of the other two MAE with DES samples, ChCl:LA and ChCl:CA:H_2O, were performed using a scanning electron microscope (Zeiss E Evo 40, Oberkochen, Germany). Images were registered at 100x magnification.

Fourier transform infrared spectroscopy (FTIR)

ATR-FTIR spectra were recorded using a Bruker Analitik IFS 66 FTIR spectrometer (Ettlingen, Germany) equipped with an ATR accessory. Samples were placed directly on the ATR crystal area and spectra were recorded in the absorbance mode from 4000 to 500 cm^{-1}, at 64 scans and 4 cm^{-1} resolution, and they were further corrected against the background spectrum of air.

X-ray diffraction (XRD) analysis

The XRD patterns of the extracted samples were recorded on a Bruker (Billerica, MA, USA) D8-Advance diffractometer equipped with a Goebel mirror for non-planar samples, a high-temperature chamber (up to 900 ºC), a KRISTALLOFLEX K760-80F X-ray generator (3000 W power, 20-60 kV voltage, and 5-80 mA current), and an X-ray tube with a copper anode. Data were recorded using Cu-Kα radiation (1.5406 Å) at room temperature and scattering angles (2θ) ranging from 2.5° to 80° (step size = 0.05º min^{-1}). The Segal method was used to calculate the crystallinity index (CI) of cellulose-based materials with the following equation (Wang et al. 2020):

$$Crystallinity\ index = \frac{I_{200} - I_{am}}{I_{200}}\ X\ 100\%$$

Where I_{200} is the maximum X-ray diffraction peak intensity at 2θ = 22-23° and I_{am} is the minimum intensity corresponding to the peak at 2θ = 18°, which corresponds to the amorphous region.

Thermogravimetric analysis

A TGA/SDTA 851 Mettler Toledo instrument (Mettler-Toledo, Schwarzenbach, Switzerland) was used to conduct thermogravimetric analysis (TGA). Dynamic testing was performed across a temperature range of 25 to 700 ºC with a heating rate 10 ºC min^{-1}. The experiments were conducted in a nitrogen atmosphere (50 mL min^{-1}) to avoid deterioration by thermal oxidation. The TGA/DTG curves yielded three parameters: the initial degradation temperature (T_i) corresponding to a 5% weight loss; the temperature (T_{max}) at which the breakdown rate is the highest; and the residual mass (%) at 700 ºC. The measurements were conducted three times for each sample.

Results and Discussion

Particle size distribution of OWP

The particle size distribution of OWP that was further used for extraction procedures is shown in Fig. 3. Results indicated that the average particle size was 332 µm, showing that the major part of the OWP

used in this study was homogeneous enough to permit the efficient extraction of the target compounds and chemicals.

Chemical Composition of OWP

The chemical composition of OWP is reported in Table 1, including holocellulose, α-Cellulose, Klason lignin, extractives, and moisture content, in those samples treated with the TAPPI standard processes. In the CP, similar composition was found, with holocellulose, α-Cellulose, and lignin contents. These results are coincident with previous studies conducted on similar plants, which also found the presence of α-cellulose (31.5 wt%), hemicellulose (11.3 wt%), lignin (23.5 wt%), extractives (27.6 wt%), and ash content (1.4 wt%) in residual biomass from olive trees (Garcia-Maraver et al. 2013). Additionally, cellulose (52.9–55.2 wt%), hemicellulose (6.7–9.9 wt%), and lignin (34.4–36.3 wt%) were extracted from olive pomace using an alkali-based process (Han and Geng 2023). Jiménez et al. revealed that the α-cellulose content of olive tree pruning was 35.7 wt%, while the holocellulose content was 61.5 wt% and the lignin content was 19.7 wt% (Jiménez et al. 2001). Similarly, Requejo et al. found that the α-cellulose content was 38.4 wt%, the holocellulose content was 66.1 wt%, the lignin content was 17.5 wt%, the extractives content was 12.4 wt%, and the ash content was 3.5 wt% (Requejo et al. 2012). In our study, the olive wood exhibited a higher concentration of α-cellulose and lignin, as shown by using both methods. These findings are consistent with previous studies (Rowell et al. 2005).

Table 1
Composition of olive wood (n = 3, mean ± SD).

Parameter	TAPPI Process Fraction (wt %)	CP Fraction (wt %)
Holocellulose	54.5 ± 0.6	51 ± 3
α-Cellulose	39.0 ± 0.6	35.5 ± 1.1
Hemicellulose	15.5 ± 0.6	15.1 ± 1.1
Klason Lignin	24 ± 2	23.3 ± 0.8
Solvent Extractives	14.0 ± 0.2	-
Ash Content	1.5 ± 0.6	-
Moisture Content	5.5 ± 0.6	-

Furthermore, the cellulose recovered from OWP by using both procedures is comparable to the cellulose obtained from other agricultural by-products, such as rice (36.9 wt%), wheat (43.0 wt%), and barley straw (39.2 wt%) (Oun and Rhim 2016). Therefore, this secondary product from OWP has the capacity to serve as a source to produce cellulose-based biocomposites. The lignin content obtained by using the TAPPI process (24.5 wt%) and CP (23.3 wt%) were higher compared to that of olive tree pruning (16.6 wt%) (Ballesteros et al. 2011) as well as than those reported by Requejo et al. for various materials, such as

cotton stalks (18.3 wt%), eucalyptus residues (17.9 wt%), sunflower seed husk (17.3 wt%), olive stones (19.1 wt%), wheat straw (14.5 wt%), sunflower stalks (14.1 wt%), and holm oak residues (13.9 wt%). According to the TAPPI process, the extractable contents of the OWP sample were higher (14.0 wt%) than those reported for olive stones (12.2 wt%) (Jiménez and González 1991) and eucalyptus globulus wood (2.4 wt%) (Romaní et al. 2011). On the contrary, the ash content of the OWP sample (1.5 wt%) was lower than that of the olive tree (3.4 wt%) (Ballesteros et al. 2011). These values agreed with those found in olive stones, holm oak, and eucalyptus residues, which ranged from 1.1 wt% to 2.4 wt% (Jiménez and González 1991).

Cellulose content with the effect of temperature in MAE with DES

The influence of the reaction temperature on the extraction of cellulose using ChCl:LA and ChCl:CA:H_2O was investigated. Table 2 displays the cellulose content obtained by MAE with different DES compositions at various temperatures already reported in the Experimental section. When the extractions were conducted at 100°C using ChCl:LA, a cellulose yield of 25.4 wt% was obtained. The increase in the extraction temperature resulted in a significant rise in the quantity of extracted cellulose. Specifically, a yield of 34.3 wt% was achieved at 120°C, while a yield of 47.8 wt% was reached at 130°C, resulting in an increase in the cellulose yield of 22.4 wt% at 130°C. A similar behaviour with the temperature increase was observed when using a ChCl:CA:H_2O mixture. Indeed, when the extractions were conducted at 100°C, a cellulose yield of 24.2 wt% was obtained, while at temperatures of 120°C and 130°C, the yield achieved was 32.5 wt% and 45.6 wt% respectively, resulting in the increase of 21.4 wt% in the cellulose yield when the temperature is set at 130 ºC. According to these results, it can be concluded that the extraction of cellulose was facilitated by high temperatures, caused by the decrease in the DES viscosity at high temperatures, which results in the decrease of limitations for mass transfer, which ultimately leads to enhanced interactions between OWP and DES (Kohli et al. 2020; Almeida et al. 2023). Therefore, it was determined that an optimal reaction temperature is necessary to maximize yields in cellulose extraction from waste OWP, while also ensuring that the recovered cellulose is not damaged by high temperatures under any circumstances. Since the higher quantity of cellulose was extracted at this temperature with no damage to the obtained material, all subsequent extractions were carried out at 130 ºC.

Table 2
Cellulose content by using MAE with DES compositions at different temperatures.

DES Composition	MAE conditions	Solid Residue (Cellulose) yield (wt%)
ChCl:LA (1:4)	Temp: 100 ºC Time: 20 min	25.4
ChCl:LA (1:4)	Temp: 120 ºC Time: 20 min	34.3
ChCl:LA (1:4)	Temp: 130 ºC Time: 20 min	47.8
ChCl:CA:H_2O (1:1:6)	Temp: 100 ºC Time: 20 min	24.2
ChCl:CA:H_2O (1:1:6)	Temp: 120 ºC Time: 20 min	32.5
ChCl:CA:H_2O (1:1:6)	Temp: 130 ºC Time: 20 min	45.6

SEM analysis

Figure 4 (a-e) depicts the SEM micrographs of cellulose samples that have undergone different extraction treatments. The untreated OWP (Fig. 4a) exhibits a smooth and compact structure ascribed to the presence of cellulose, hemicellulose, lignin, pectin, and impurities such as waxes, ashes, and natural oils (Bouhamed et al. 2020; Azlan et al. 2022; Valdés et al. 2023). The analysis of TPC, (Fig. 4b) and CPC (Fig. 4c), demonstrates that cellulose remains but undergoes a loss of the smooth surface, resulting in an uneven morphology (Rizwan et al. 2021; Asif et al. 2022) caused by the solvents treatment to remove extractives (Kian et al. 2020b) and the further alkaline treatment to eliminate residual lignin and hemicelluloses.

In ChCl:LA (Fig. 4d) and ChCl:CA:H_2O (Fig. 4e), a rough surface area with some holes was visible. This may be due to the microwave irradiation of DES at high temperatures, with the consequent removal of lignin, hemicelluloses and extractives. The use of DES results in cellulose swelling and formation of hydrogen bonds. This is because microwaves produce heat and accelerate chemical processes, which could potentially alter the cellulose structure and morphology, with the result of a significant portion of non-cellulosic components successfully removed (Yu et al. 2020). The use of microwave extraction with DES resulted in the disruption of the lignocellulosic complex (Figs. 4d and 4e), leading to the reduction in length of the fibers, and lignin and hemicelluloses extraction. These characteristics reveal a greater level of porosity and a broader surface area of the cellulose (Sharma and Dash 2021; Azlan et al. 2022; Kwon

et al. 2023). Based on the analysis of the SEM images, it can be concluded that the cellulose extraction using MAE with DES required less chemicals and lower times compared to the CP method.

FTIR analysis

Figure 5 shows the FTIR spectra in the absorbance mode of all types of cellulose extracted by different procedures in this study. All spectra showed similar peaks and bands corresponding to cellulose functional groups, but some significant features can be observed since extraction with the TAPPI and conventional protocols showed some differences with results obtained with MAE using DES. Table 3 details the main peaks observed in all cases.

Table 3
Assignment of peaks in the FTIR analysis of TPC, CPC, ChCl:LA and ChCl:CA:H_2O samples (all wavelength values in cm^{-1})

TPC	CPC	ChCl:LA	ChCl:CA:H_2O	Assignments	Ref.
3328	3328	3328	3328	-OH intermolecular and intramolecular stretching	(Javier-Astete et al. 2021)
2890	2890	2890	2890	-CH and -CH_2 stretching of methyl and methylene groups	(Rodríguez et al. 2023)
1725	1725	1725	1725	Acetyl or carboxylic acid stretching with free -COOH carboxyl groups (hemicellulose)	(Souissi et al. 2022)
1609	1616	-	-	Bending of absorbed water in the H-O-H position	(Ndruru et al. 2019)
-	-	1593	1586	Skeletal vibration of aromatics (lignin)	(Souissi et al. 2022)
-	-	1499	1499	C = C aromatic ring of lignin	(Zhuang et al. 2020)
-	-	1454	1447	Skeletal vibration of aromatics (lignin)	(Souissi et al. 2022)
-	-	1418	1425	Skeletal vibration of aromatics (lignin)	(Yu et al. 2022)
1374	1367	-	-	-CH groups wagging vibrations	(Souissi et al. 2022)
1315	1315	1315	1315	-CH_2 wagging	(Traoré et al. 2018)
1235	1228	1228	1228	C-O stretching in cellulose	(Souissi et al. 2022)
1147	1155	1155	1155	C-O-C asymmetric stretching in cellulose	(Vârban et al. 2021)
1023	1023	1023	1023	C-O stretching in cellulose	(Han and Geng 2023)
891	891	891	891	C1-H deformation (β-(1.4)-glycosidic bonds)	(Javier-Astete et al. 2021)

A broad absorption peak corresponding to -OH intermolecular and intramolecular stretching vibrations is centered at 3328 cm^{-1} for all four samples (Candido and Gonçalves 2016; Kian et al. 2020a). The absorption peak at 2890 cm^{-1} corresponds to the -CH_3 and -CH_2 stretching vibrations of methyl and methylene groups respectively, and it is indicative of the highly crystalline cellulose structure (Hachaichi et al. 2021), which suggests that the extractives were successfully removed from all samples (Wulandari

et al. 2016; Traoré et al. 2018). The peak at 1725 cm^{-1} represents the -C = O vibration in the O = C-OH free carboxyl groups stretching of acetyl or carboxylic acid groups of the glucuronic acid unit, typical of hemicellulose in all samples (Abdel et al. 2015; Sánchez-Gutiérrez et al. 2020). By the presence of this peak, it can be concluded that hemicellulose remained in all samples after alkali and microwave treatments. The peaks observed in TPC and CPC samples at 1609 cm^{-1} and 1616 cm^{-1}correspond to the H-O-H bending vibrations of absorbed water molecules, which explains the hydrophilic properties of the cellulosic materials (Nagarajan et al. 2021). This result also indicates that there was no longer any lignin in TPC and CPC samples, which is confirmed by the absence of a particular peak ranging between 1418 and 1593 cm^{-1} (Kian et al. 2020a). It is noticeable that the alkali treatment, in particular, substantially disrupted the cellulose-lignin linkages, resulting in a more prone extraction of lignin (Abdel et al. 2015; Nagarajan et al. 2021). However, in ChCl:LA and ChCl:CA:H_2O samples, peaks at 1418–1593 cm^{-1} were observed respectively, due to the presence of lignin, particularly in a peak centered at 1499 cm^{-1}, representing aromatic C = C stretching of the benzene ring, which is characteristic of lignin. For both MAE samples, it was observed that peaks at 1418 cm^{-1}, 1454 cm^{-1} and 1593 cm^{-1} corresponded to the skeletal vibrations of the aromatic (lignin) groups. Peaks at 1367 cm^{-1} and 1374 cm^{-1} for the-C-H bending vibrations were also observed for both, TPC and CPC samples (Ibrahim and Osman 2009; Hachaichi et al. 2021). Peaks at 1315 cm^{-1} were observed for all samples and they can be attributed to -CH_2 wagging vibrations (Rosa et al. 2012; Hachaichi et al. 2021) as well as the -O-H bending vibrations (Kalita et al. 2013). Peaks at 1235 cm^{-1} (TPC sample) and 1228 cm^{-1} (CPC, ChCl:LA & ChCl:CA:H_2O) represents the characteristic -C-O stretching and -O-H in-plane vibrations of polysaccharides (Pecoraro et al. 2022), as well as -C-O- stretching of the carboxyl group of cellulose (Sánchez-Gutiérrez et al. 2020), while peaks at 1147 cm^{-1} (TPC) and 1155 cm^{-1} (CPC, ChCl:LA and ChCl:CA:H_2O) are associated with the C-O-C asymmetric stretching vibration of the pyranose ring skeleton of cellulose (Traoré et al. 2018; Kian et al. 2020b). In all samples, a sharp absorbance peak of the-C-O- stretching vibration appeared at 1023 cm^{-1}, whereas the peak observed at 891 cm^{-1} corresponded to -CH_2 groups in β-(1,4) glycosidic linkages between the glucose monomers (Sánchez-Gutiérrez et al. 2020), which exposes the common structural chemistry of cellulose molecules (Chen et al. 2018; Jurado-Contreras et al. 2023) and C1-H deformation (Han and Geng 2023). In conclusion, and after the FTIR analysis, it can be drawn that the cellulose extraction from waste OWP by using microwave with DES was successful.

XRD analysis

The XRD patterns of the extracted samples are shown in Fig. 6, while Table 4 shows the most relevant results obtained for all samples. It can be seen that the OWP samples extracted by the different treatment protocols have identical diffraction peaks, typical from cellulose. Based on the peaks position, the structure of the extracted cellulose can be classified as cellulose type I (Isci et al. 2020; Jurado-Contreras et al. 2023). The highest peak for all samples indicated the primary crystalline constitution of cellulose I, which is observed at 2θ = 22.44° and 2θ = 22.27° (Kian et al. 2020a). The small peak at 2θ = 34.79° also indicated that samples had a natural cellulose I structure (Han and Geng 2023). The peak

shapes of the differently treated samples remained identical, indicating that the different treatments (TPC, CPC, and MAE/DES) did not change the crystalline structure of the cellulose samples. This result can be explained by the formation of intra- and intermolecular hydrogen bonding, leading to the formation of highly organized cellulose crystallites (Kian et al. 2020b). The intensity of the peak at 2θ = 22.09° to 22.44° was different, depending of the samples treatment, suggesting that hemicellulose and lignin in the amorphous regions were eliminated, resulting in the increase of the cellulose crystallinity (Kale et al. 2018; Hachaichi et al. 2021). In general terms, the crystallinity index values increased in proportion to the number of amorphous components removed, as expected. It may be said that in samples extracted by TPC, CPC and MAE/DES with LA, the process removed the maximum portion of hemicellulose and lignin. Furthermore, a maximum crystallinity index of 72.89% was found in the TPC sample compared to the CPC and MAE samples. This is likely explained since the TPC method is a well-maintained process for cellulose extraction and may result in a higher yield of crystalline cellulose. The lowest crystallinity index was obtained by MAE using the ChCl:LA and ChCl:CA:H_2O samples (68.22% and 66.69%, respectively). This effect can be caused by the greater structural changes in the material structure caused by microwaves during cellulose extraction, joined to the presence of some amounts of lignin and hemicellulose in the cellulose structure (Han and Geng 2023), resulting in overall lower crystallinity (Isci et al. 2020). This enables these materials to be utilized as biofillers for composites to provide outstanding mechanical properties (Hussin et al. 2016).

Table 4
Crystallinity index and 2(theta) of different cellulose materials

Sample	2 (theta) (degree)	Crystallinity index (%)
TPC	22.27	72.89
CPC	22.44	70.30
ChCl:LA	22.27	68.22
ChCl:CA:H_2O	22.09	66.69

Thermogravimetric analysis

The TGA and derivative (DTG) curves for cellulose extracted by using different methods are shown in Figs. 7a and 7b respectively. All samples showed initial decomposition steps at low temperatures, caused by the dehydration process, in which moisture or some other volatile substances were evaporated (Garcia-Maraver et al. 2013). Differences in mass losses in this initial decomposition step were mainly dependent on the initial moisture content of the samples. It was already discussed that the TPC and CPC samples were almost extractive-free and had a higher cellulose content (Kian et al. 2020b). Therefore, the initial degradation temperatures at 5% weight loss (236°C and 241°C, respectively) were higher than those of the ChCl:LA and ChCl:CA:H_2O samples (210°C and 218°C, respectively) (Fig. 7a). This suggests that the initial stages of the cellulose thermal degradation occur at different temperatures, with ChCl:LA starting to degrade at a lower temperature even if compared with

ChCl:CA:H_2O samples. This may be due to the presence of residual amounts of hemicellulose and extractives in the case of MAE/DES samples, which absorb moisture and may promote degradation at lower temperatures (Poletto et al. 2014; Rodríguez et al. 2023).

Table 5
Thermal degradation temperatures and residual mass at 700 ºC of different samples. All samples were analysed in triplicate

Samples	T_i (ºC) 5% wt. loss	Maximum decomposition Temperature (ºC), T_{max}	Residual mass at 700ºC (%)
TPC	236 ± 2	347 ± 1	32 ± 2
CPC	241 ± 4	360 ± 11	26 ± 1
ChCl:LA	211 ± 3	386 ± 5	19 ± 1
ChCl:CA:H_2O	219 ± 8	372 ± 4	22 ± 1

Dehydration, decarboxylation, and depolymerization of glycosidic bonds in the cellulose structure are the primary causes of the second stage in the thermal degradation of these materials, which starts (5% weight loss) between 211°C and 241°C and has the maximum degradation rate between 347 ºC and 386 ºC. This stage involves degradation of cellulose, hemicellulose, and lignin (Trache et al. 2016; Ndruru et al. 2019). The material more prone to be degraded is hemicellulose, which typically breaks down between 220 ºC and 315°C. The random amorphous structure of hemicellulose, which is composed of a variety of sugars, makes it simple to break down into volatile compounds such as CO and CO_2 (Yang et al. 2007; Morán et al. 2008). In comparison, cellulose is composed of long, orderly chains of unbranched glucose, and crystalline regions improve the thermal stability, as opposed to hemicellulose's branched glucose molecules (Yang et al. 2006; Han and Geng 2023). The temperature range for thermal breakdown in cellulose is 300–400°C, and it can be concluded that the higher thermal degradation temperature corresponds to the higher purity of cellulose structures. It can be observed that the maximum decomposition temperature differed significantly among the four samples, with ChCl:LA being the most thermally stable (having the highest temperature at 386°C) and TPC being the least thermally stable (having the lowest temperature at 347°C). This tendency may be related to the crystalline index of the ChCl:LA samples (Poletto et al. 2014; Azum et al. 2021). Oxidation and breakdown of carbonized waste primarily occur at 400–700°C during the third stage of degradation (Sánchez-Gutiérrez et al. 2020). At this point, lignin begins to break down and slows the process, resulting in higher degradation temperatures. Lignin's thermal degradation is a slow process and can occur anywhere between 150°C and 700°C due to the high number of aromatic rings it contains. This behavior was confirmed in the DTG curve (Fig. 7b), where the ChCl:LA and ChCl:CA:H_2O samples showed comparatively higher peak decomposition temperatures because the cellulose compartment is thermally stable. It is likely that the presence of amorphous characteristic compounds in the TPC and CPC samples could speed up their degradation (Kian et al. 2020a). A sharp peak in the DTG curve was observed in the ChCl:LA samples compared to the other three types of samples, which may indicate the higher cellulose purity in the

ChCl:LA samples (Taflick et al. 2017). From 400 ºC on, the ChCl:LA and ChCl:CA:H_2O samples constantly reduced in weight.

Finally, there were differences in the residual weight of samples (Table 5), with TPC having the highest value (32%), and ChCl:LA having the lowest value (19%). This suggests that these materials show different degrees of char-forming capacity, with TPC having the highest and ChCl:LA the lowest capacity. Additionally, the char residue served as a thermal barrier, which enhanced thermal stability (Nukala et al. 2022). These results indicated that ChCl:LA produced the most thermally stable and slowest degrading sample, whereas CPC produced the least thermally stable and fastest-degrading sample.

Comparison between CP and MAE process

Results obtained from the conventional extraction process using an ethanol:toluene mixture with alkali treatment were compared to those obtained by MAE using DES (ChCl:LA and ChCl:CA:H_2O) as suitable and sustainable solvents. This comparison indicated that both methods yielded comparable results, but there is a difference in time, temperature, and use of chemicals between both methods. The most important difference between the MAE process and the CP is that MAE requires short processing times with only the presence of the solvent (in this case DES), as opposed to solvents and other chemicals in CP. Furthermore, it is essential to take into consideration that MAE is capable of producing extracts with a cellulose content comparable to that of extracts produced via CP. Nevertheless, MAE has some drawbacks, since requires expensive equipment that may not be available in all laboratories. However, the operational costs are cheaper in comparison to CP. Microwave power, irradiation time, and sample size must be controlled for optimal cellulose extraction to avoid damaging the extracted products, sample overheating and degradation that should be monitored.

Conclusion

The results of this study open the door to the potential of applying a MAE/DES approach that is not only simpler to use but also more favorable to the environment than CP to extract cellulose from waste OWP, resulting in a very effective and ecologically-sound technique. By using DES, the extraction procedure achieved a significant reduction in toxicity and waste generation, while achieving similar extraction yields and purities to CP. Microwave irradiation enhances the efficiency of the process by facilitating a reduction in extraction time, energy consumption, and solvent use. The method has shown effective in extracting cellulose from the waste OWP, and characterization techniques confirmed that the purity of the extracted cellulose is also comparable with cellulose obtained by CP. The morphology study depicts some pores that were found in MAE/DES extracted cellulose. Through FTIR analysis, it was shown that the cellulose products extracted from waste OWP had the relevant functional groups that are associated with pure cellulose. The XRD investigation revealed that the cellulose product had a crystalline structure of cellulose-I, with a 2θ value of 22.3º and a crystallinity index of 68.2% which is also comparable with results for CP cellulose. The thermal stability of the MAE/DES cellulose is excellent, as shown by a maximum decomposition temperature of 386 ºC. MAE/DES cellulose may be used in many applications,

including textiles, packaging, medicine, cosmetics, and the production of bio-based materials. The use of an ecologically sustainable technique for cellulose extraction has great potential in promoting the development of the circular economy. Further studies to go deeper into modifications of MAE to overcome its limitations and enhance its acceptance as a technology in the future will be performed to extend this study to other important biomaterials.

Declarations

Declarations

Ethical Approval

Not applicable

Funding

This work was funded by the Spanish Ministry of Science and Innovation and the Spanish Research Agency (Ref. PID2020-116496RB-C21). This study forms part of the Advanced Materials programme and was supported by MCIN with funding from European Union NextGenerationEU (PRTR-C17.I1) and by Generalitat Valenciana (Ref. MFA/2022/061). This work was also funded by Innovative Doctoral Scholarship from the Development and Cohesion Fund (FSC)-Extract Plan Research and Innovation 2015–2017.

Author Contribution

M.M.A. perfomed the experimental study under the supervision of A.G., C.E.C.. M.C.G. and A.J. M.M.A. wrote the main manuscript text andA.G., C.E.C.. M.C.G. and A.J reviewed the manuscript.

References

1. Abdel HE, Alanazi H, Alghamdi A (2015) Extraction and bleaching of olive tree branch cellulose. Bioresources 10:7136–7150. https://doi.org/10.15376/biores.10.4.7136-7150
2. Alam MM, Greco A, Rajabimashhadi Z, Esposito Corcione C (2024) Efficient and environmentally friendly techniques for extracting lignin from lignocellulose biomass and subsequent uses: A review. Cleaner Materials 13:100253. https://doi.org/10.1016/j.clema.2024.100253
3. Almeida RO, Maloney TC, Gamelas JAF (2023) Production of functionalized nanocelluloses from different sources using deep eutectic solvents and their applications. Industrial Crops and Products 199:116583. https://doi.org/10.1016/j.indcrop.2023.116583
4. Azlan NSM, Yap CL, Gan S, Rahman MBA (2022) Effectiveness of various solvents in the microwave-assisted extraction of cellulose from oil palm mesocarp fiber. Materials Today: Proceedings

59:583–590. https://doi.org/10.1016/j.matpr.2021.12.086

5. Azum N, Jawaid M, Kian LK, et al (2021) Extraction of Microcrystalline Cellulose from Washingtonia Fibre and Its Characterization. Polymers 13:3030. https://doi.org/10.3390/polym13183030
6. Ballesteros I, Ballesteros M, Cara C, et al (2011) Effect of water extraction on sugars recovery from steam exploded olive tree pruning. Bioresource Technology 102:6611–6616. https://doi.org/10.1016/j.biortech.2011.03.077
7. Boli E, Prinos N, Louli V, et al (2022) Recovery of Bioactive Extracts from Olive Leaves Using Conventional and Microwave-Assisted Extraction with Classical and Deep Eutectic Solvents. Separations 9:255. https://doi.org/10.3390/separations9090255
8. Bouhamed N, Souissi S, Marechal P, et al (2020) Physicochemical, Morphological and Thermal Characterization of Composites Based on Olive Wood Flour. pp 259–263. https://doi.org/10.1007/978-3-030-52071-7_36
9. Candido RG, Gonçalves AR (2016) Synthesis of cellulose acetate and carboxymethylcellulose from sugarcane straw. Carbohydrate Polymers 152:679–686. https://doi.org/10.1016/j.carbpol.2016.07.071
10. Chadni M, Bals O, Ziegler-Devin I, et al (2019) Microwave-assisted extraction of high-molecular-weight hemicelluloses from spruce wood. Comptes Rendus Chimie 22:574–584. https://doi.org/10.1016/j.crci.2019.07.002
11. Chen W, He H, Zhu H, et al (2018) Thermo-Responsive Cellulose-Based Material with Switchable Wettability for Controllable Oil/Water Separation. Polymers (Basel) 10:592. https://doi.org/10.3390/polym10060592
12. Esposito Corcione C, Striani R, Ferrari F, et al (2020) An Innovative Method for the Recycling of Waste Carbohydrate-Based Flours. Polymers (Basel) 12:E1414. https://doi.org/10.3390/polym12061414
13. Ferrari F, Striani R, Fico D, et al (2022) An Overview on Wood Waste Valorization as Biopolymers and Biocomposites: Definition, Classification, Production, Properties and Applications. Polymers 14:5519. https://doi.org/10.3390/polym14245519
14. Galbe M, Wallberg O (2019) Pretreatment for biorefineries: a review of common methods for efficient utilisation of lignocellulosic materials. Biotechnol Biofuels 12:294. https://doi.org/10.1186/s13068-019-1634-1
15. Garcia-Maraver A, Salvachúa D, Martínez MJ, et al (2013) Analysis of the relation between the cellulose, hemicellulose and lignin content and the thermal behavior of residual biomass from olive trees. Waste Management 33:2245–2249. https://doi.org/10.1016/j.wasman.2013.07.010
16. Gullón B, Gullón P, Eibes G, et al (2018) Valorisation of olive agro-industrial by-products as a source of bioactive compounds. Science of The Total Environment 645:533–542. https://doi.org/10.1016/j.scitotenv.2018.07.155
17. Hachaichi A, Kouini B, Kian LK, et al (2021) Extraction and Characterization of Microcrystalline Cellulose from Date Palm Fibers using Successive Chemical Treatments. J Polym Environ 29:1990–

1999. https://doi.org/10.1007/s10924-020-02012-2

18. Haldar D, Purkait MK (2021) A review on the environment-friendly emerging techniques for pretreatment of lignocellulosic biomass: Mechanistic insight and advancements. Chemosphere 264:128523. https://doi.org/10.1016/j.chemosphere.2020.128523
19. Han W, Geng Y (2023) Optimization and characterization of cellulose extraction from olive pomace. Cellulose. https://doi.org/10.1007/s10570-023-05195-8
20. Hussin MH, Pohan NA, Garba ZN, et al (2016) Physicochemical of microcrystalline cellulose from oil palm fronds as potential methylene blue adsorbents. International Journal of Biological Macromolecules 92:11–19. https://doi.org/10.1016/j.ijbiomac.2016.06.094
21. Ibrahim M, Osman O (2009) Spectroscopic Analyses of Cellulose: Fourier Transform Infrared and Molecular Modelling Study. Journal of Computational and Theoretical Nanoscience 6:1054–1058. https://doi.org/10.1166/jctn.2009.1143
22. Isci A, Erdem GM, Bagder Elmaci S, et al (2020) Effect of microwave-assisted deep eutectic solvent pretreatment on lignocellulosic structure and bioconversion of wheat straw. Cellulose 27:8949–8962. https://doi.org/10.1007/s10570-020-03371-8
23. Javier-Astete R, Jimenez-Davalos J, Zolla G (2021) Determination of hemicellulose, cellulose, holocellulose and lignin content using FTIR in Calycophyllum spruceanum (Benth.) K. Schum. and Guazuma crinita Lam. PLOS ONE 16:e0256559. https://doi.org/10.1371/journal.pone.0256559
24. Jiménez L, González F (1991) Study of the physical and chemical properties of lignocellulosic residues with a view to the production of fuels. Fuel 70:947–950. https://doi.org/10.1016/0016-2361(91)90049-G
25. Jiménez L, Pérez I, García JC, Rodríguez A (2001) Influence of process variables in the ethanol pulping of olive tree trimmings. Bioresour Technol 78:63–69. https://doi.org/10.1016/s0960-8524(00)00165-6
26. Jurado-Contreras S, Navas-Martos FJ, García-Ruiz Á, et al (2023) Obtaining Cellulose Nanocrystals from Olive Tree Pruning Waste and Evaluation of Their Influence as a Reinforcement on Biocomposites. Polymers 15:4251. https://doi.org/10.3390/polym15214251
27. Kale RD, Bansal PS, Gorade VG (2018) Extraction of Microcrystalline Cellulose from Cotton Sliver and Its Comparison with Commercial Microcrystalline Cellulose. J Polym Environ 26:355–364. https://doi.org/10.1007/s10924-017-0936-2
28. Kalita RD, Nath Y, Ochubiojo ME, Buragohain AK (2013) Extraction and characterization of microcrystalline cellulose from fodder grass; Setaria glauca (L) P. Beauv, and its potential as a drug delivery vehicle for isoniazid, a first line antituberculosis drug. Colloids and Surfaces B: Biointerfaces 108:85–89. https://doi.org/10.1016/j.colsurfb.2013.02.016
29. Khandanlou R, Ngoh G, Chong WT (2016) Feasibility Study and Structural Analysis of Cellulose Isolated from Rice Husk: Microwave Irradiation, Optimization, and Treatment Process Scheme. Bioresources 11:. https://doi.org/10.15376/biores.11.3.5751-5766

30. Kian LK, Saba N, Jawaid M, et al (2020a) Properties and characteristics of nanocrystalline cellulose isolated from olive fiber. Carbohydrate Polymers 241:116423. https://doi.org/10.1016/j.carbpol.2020.116423
31. Kian LK, Saba N, Jawaid M, Fouad H (2020b) Characterization of microcrystalline cellulose extracted from olive fiber. International Journal of Biological Macromolecules 156:347–353. https://doi.org/10.1016/j.ijbiomac.2020.04.015
32. Kłosowski G, Mikulski D, Lewandowska N (2020) Microwave-Assisted Degradation of Biomass with the Use of Acid Catalysis. Catalysts 10:641. https://doi.org/10.3390/catal10060641
33. Kohli K, Katuwal S, Biswas A, Sharma BK (2020) Effective delignification of lignocellulosic biomass by microwave assisted deep eutectic solvents. Bioresource Technology 303:122897. https://doi.org/10.1016/j.biortech.2020.122897
34. Kwon G-J, Bandi R, Yang B-S, et al (2021) Choline chloride based deep eutectic solvents for the lignocellulose nanofibril production from Mongolian oak (Quercus mongolica). Cellulose 28:9169–9185. https://doi.org/10.1007/s10570-021-04102-3
35. Kwon G-J, Cho S-W, Bandi R, et al (2023) Production of lignocellulose nanofibrils by conventional and microwave-assisted deep-eutectic-solvent pretreatments: mechanical, antioxidant, and UV-blocking properties. Cellulose 30:4277–4292. https://doi.org/10.1007/s10570-023-05164-1
36. Leite ALMP, Zanon CD, Menegalli FC (2017) Isolation and characterization of cellulose nanofibers from cassava root bagasse and peelings. Carbohydrate Polymers 157:962–970. https://doi.org/10.1016/j.carbpol.2016.10.048
37. Mamilla JLK, Novak U, Grilc M, Likozar B (2019) Natural deep eutectic solvents (DES) for fractionation of waste lignocellulosic biomass and its cascade conversion to value-added bio-based chemicals. Biomass and Bioenergy 120:417–425. https://doi.org/10.1016/j.biombioe.2018.12.002
38. Morán JI, Alvarez VA, Cyras VP, Vázquez A (2008) Extraction of cellulose and preparation of nanocellulose from sisal fibers. Cellulose 15:149–159. https://doi.org/10.1007/s10570-007-9145-9
39. Mujtaba M, Fernandes Fraceto L, Fazeli M, et al (2023) Lignocellulosic biomass from agricultural waste to the circular economy: a review with focus on biofuels, biocomposites and bioplastics. Journal of Cleaner Production 402:136815. https://doi.org/10.1016/j.jclepro.2023.136815
40. Nagarajan KJ, Ramanujam NR, Sanjay MR, et al (2021) A comprehensive review on cellulose nanocrystals and cellulose nanofibers: Pretreatment, preparation, and characterization. Polymer Composites 42:1588–1630. https://doi.org/10.1002/pc.25929
41. Ndruru STCL, Wahyuningrum D, Bundjali B, Arcana IM (2019) Green simple microwave-assisted extraction (MAE) of cellulose from Theobroma cacao L. (TCL) husk. IOP Conf Ser: Mater Sci Eng 541:012017. https://doi.org/10.1088/1757-899X/541/1/012017
42. Nukala SG, Kong I, Kakarla AB, et al (2022) Development of Wood Polymer Composites from Recycled Wood and Plastic Waste: Thermal and Mechanical Properties. Journal of Composites Science 6:194. https://doi.org/10.3390/jcs6070194

43. Oun AA, Rhim J-W (2016) Isolation of cellulose nanocrystals from grain straws and their use for the preparation of carboxymethyl cellulose-based nanocomposite films. Carbohydr Polym 150:187–200. https://doi.org/10.1016/j.carbpol.2016.05.020
44. Pecoraro MT, Mellinas C, Piccolella S, et al (2022) Hemp Stem Epidermis and Cuticle: From Waste to Starter in Bio-Based Material Development. Polymers 14:2816. https://doi.org/10.3390/polym14142816
45. Poletto M, Ornaghi Júnior HL, Zattera AJ (2014) Native Cellulose: Structure, Characterization and Thermal Properties. Materials (Basel) 7:6105–6119. https://doi.org/10.3390/ma7096105
46. Puligundla P, Oh S-E, Mok C (2016) Microwave-assisted pretreatment technologies for the conversion of lignocellulosic biomass to sugars and ethanol: a review. Carbon letters 17:1–10. https://doi.org/10.5714/CL.2016.17.1.001
47. Rachiero GP, Berton P, Shamshina J (2022) Deep Eutectic Solvents: Alternative Solvents for Biomass-Based Waste Valorization. Molecules 27:6606. https://doi.org/10.3390/molecules27196606
48. Rastogi M, Shrivastava S (2017) Recent advances in second generation bioethanol production: An insight to pretreatment, saccharification and fermentation processes. Renewable and Sustainable Energy Reviews 80:330–340. https://doi.org/10.1016/j.rser.2017.05.225
49. Requejo A, Rodríguez A, González Z, et al (2012) Ethanol pulping as a stage in the bio-refinery of olive tree prunings. Bioresources 7:3142–3159. https://doi.org/10.15376/biores.7.3.3142-3159
50. Rodríguez J, Navas F, Jurado-Contreras S, et al (2023) Manufacture and characterisation of polylactic acid biocomposites with high-purity cellulose isolated from olive pruning waste. Journal of Reinforced Plastics and Composites 43:073168442311622. https://doi.org/10.1177/07316844231162286
51. Romaní A, Garrote G, López F, Parajó JC (2011) Eucalyptus globulus wood fractionation by autohydrolysis and organosolv delignification. Bioresource Technology 102:5896–5904. https://doi.org/10.1016/j.biortech.2011.02.070
52. Romero-García JM, Niño L, Martínez-Patiño C, et al (2014) Biorefinery based on olive biomass. State of the art and future trends. Bioresource Technology 159:421–432. https://doi.org/10.1016/j.biortech.2014.03.062
53. Rosa SML, Rehman N, de Miranda MIG, et al (2012) Chlorine-free extraction of cellulose from rice husk and whisker isolation. Carbohydrate Polymers 87:1131–1138. https://doi.org/10.1016/j.carbpol.2011.08.084
54. Rowell RM, Pettersen R, Han JS, et al (2005) Cell wall chemistry. Handbook of wood chemistry and wood composites Boca Raton, Fla : CRC Press, 2005: pages 35-74
55. Sánchez-Gutiérrez M, Espinosa E, Bascón-Villegas I, et al (2020) Production of Cellulose Nanofibers from Olive Tree Harvest—A Residue with Wide Applications. Agronomy 10:696. https://doi.org/10.3390/agronomy10050696

56. Sharma M, Dash KK (2021) Deep eutectic solvent-based microwave-assisted extraction of phytochemical compounds from black jamun pulp. Journal of Food Process Engineering 44:e13750. https://doi.org/10.1111/jfpe.13750
57. Souissi S, Lachtar F, Elloumi A, Bergeret A (2022) Properties of wood polymer composites based on polypropylene/olive wood flour: effects of fiber treatment and compatibilizer. Iranian Polymer Journal 31:. https://doi.org/10.1007/s13726-022-01089-x
58. Taflick T, Schwendler LA, Rosa SML, et al (2017) Cellulose nanocrystals from acacia bark–Influence of solvent extraction. International Journal of Biological Macromolecules 101:553–561. https://doi.org/10.1016/j.ijbiomac.2017.03.076
59. Trache D, Hussin MH, Hui Chuin CT, et al (2016) Microcrystalline cellulose: Isolation, characterization and bio-composites application—A review. International Journal of Biological Macromolecules 93:789–804. https://doi.org/10.1016/j.ijbiomac.2016.09.056
60. Traoré M, Kaal J, Martínez Cortizas A (2018) Differentiation between pine woods according to species and growing location using FTIR-ATR. Wood Sci Technol 52:487–504. https://doi.org/10.1007/s00226-017-0967-9
61. Valdés A, Mondragon G, Garrigós MC, et al (2023) Microwave-assisted extraction of cellulose nanocrystals from almond (Prunus amygdalus) shell waste. Frontiers in Nutrition 9: https://doi.org/10.3389/fnut.2022.1071754
62. Vârban R, Crișan I, Vârban D, et al (2021) Comparative FT-IR Prospecting for Cellulose in Stems of Some Fiber Plants: Flax, Velvet Leaf, Hemp and Jute. Applied Sciences 11:8570. https://doi.org/10.3390/app11188570
63. Wang J, Jing W, Tian H, et al (2020) Investigation of Deep Eutectic Solvent-Based Microwave-Assisted Extraction and Efficient Recovery of Natural Products. ACS Sustainable Chem Eng 8:12080–12088. https://doi.org/10.1021/acssuschemeng.0c03393
64. Wise LE, Murphy M, Adieco A a. D (1946) A Chlorite Holocellulose, its Fractionation and Bearing on Summative Wood Analysis and Studies on the Hemicelluloses.
65. Wulandari WT, Rochliadi A, Arcana IM (2016) Nanocellulose prepared by acid hydrolysis of isolated cellulose from sugarcane bagasse. IOP Conf Ser: Mater Sci Eng 107:012045. https://doi.org/10.1088/1757-899X/107/1/012045
66. Yang H, Yan R, Chen H, et al (2007) Characteristics of hemicellulose, cellulose and lignin pyrolysis. Fuel 86:1781–1788. https://doi.org/10.1016/j.fuel.2006.12.013
67. Yang H, Yan R, Chen H, et al (2006) In-Depth Investigation of Biomass Pyrolysis Based on Three Major Components: Hemicellulose, Cellulose and Lignin. Energy Fuels 20:388–393. https://doi.org/10.1021/ef0580117
68. Yu J, Ramirez Reina T, Paterson N, Millan M (2022) On the primary pyrolysis products of torrefied oak at extremely high heating rates in a wire mesh reactor. Applications in Energy and Combustion Science 9:100046. https://doi.org/10.1016/j.jaecs.2021.100046

69. Yu W, Wang C, Yi Y, et al (2020) Comparison of Deep Eutectic Solvents on Pretreatment of Raw Ramie Fibers for Cellulose Nanofibril Production. ACS Omega 5:5580–5588. https://doi.org/10.1021/acsomega.0c00506
70. Zhuang J, Li M, Pu Y, et al (2020) Observation of Potential Contaminants in Processed Biomass Using Fourier Transform Infrared Spectroscopy. Applied Sciences 10:4345. https://doi.org/10.3390/app10124345

Figures

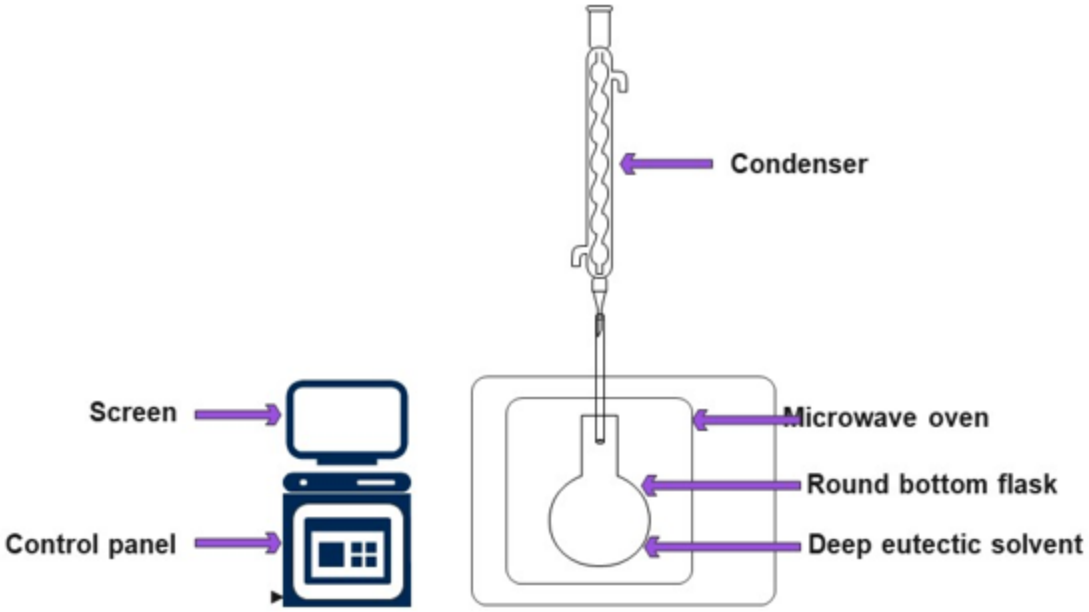

Figure 1

Scheme of a microwave oven used for DES synthesis

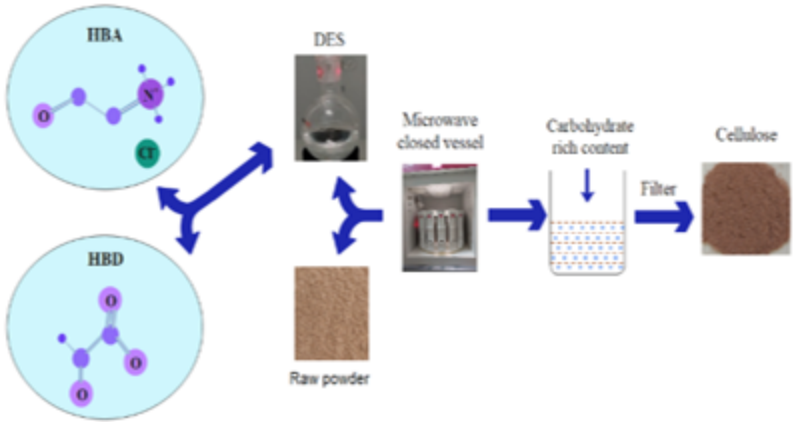

Figure 2

Scheme for the MAE process for cellulose

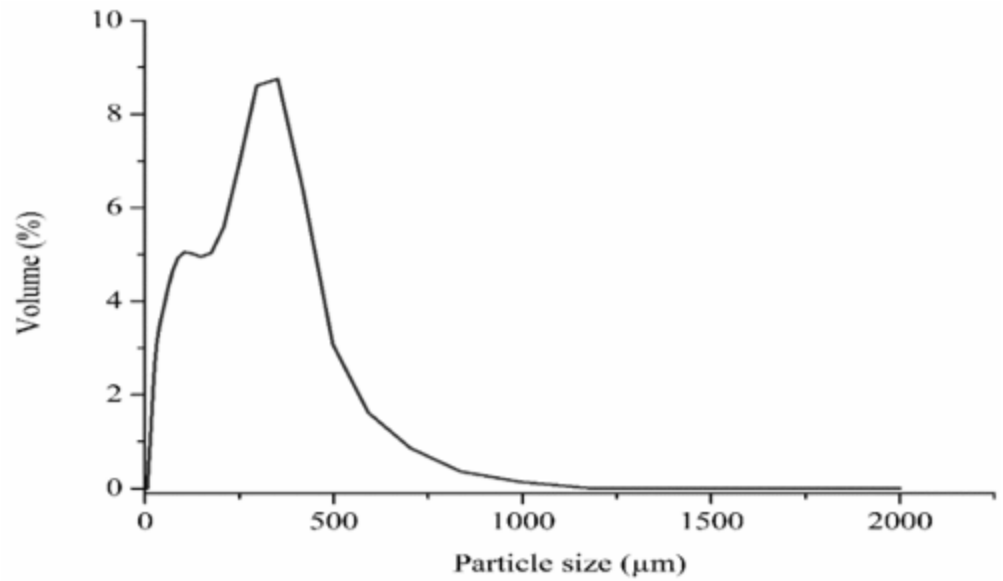

Figure 3

Particle size distribution of OWP

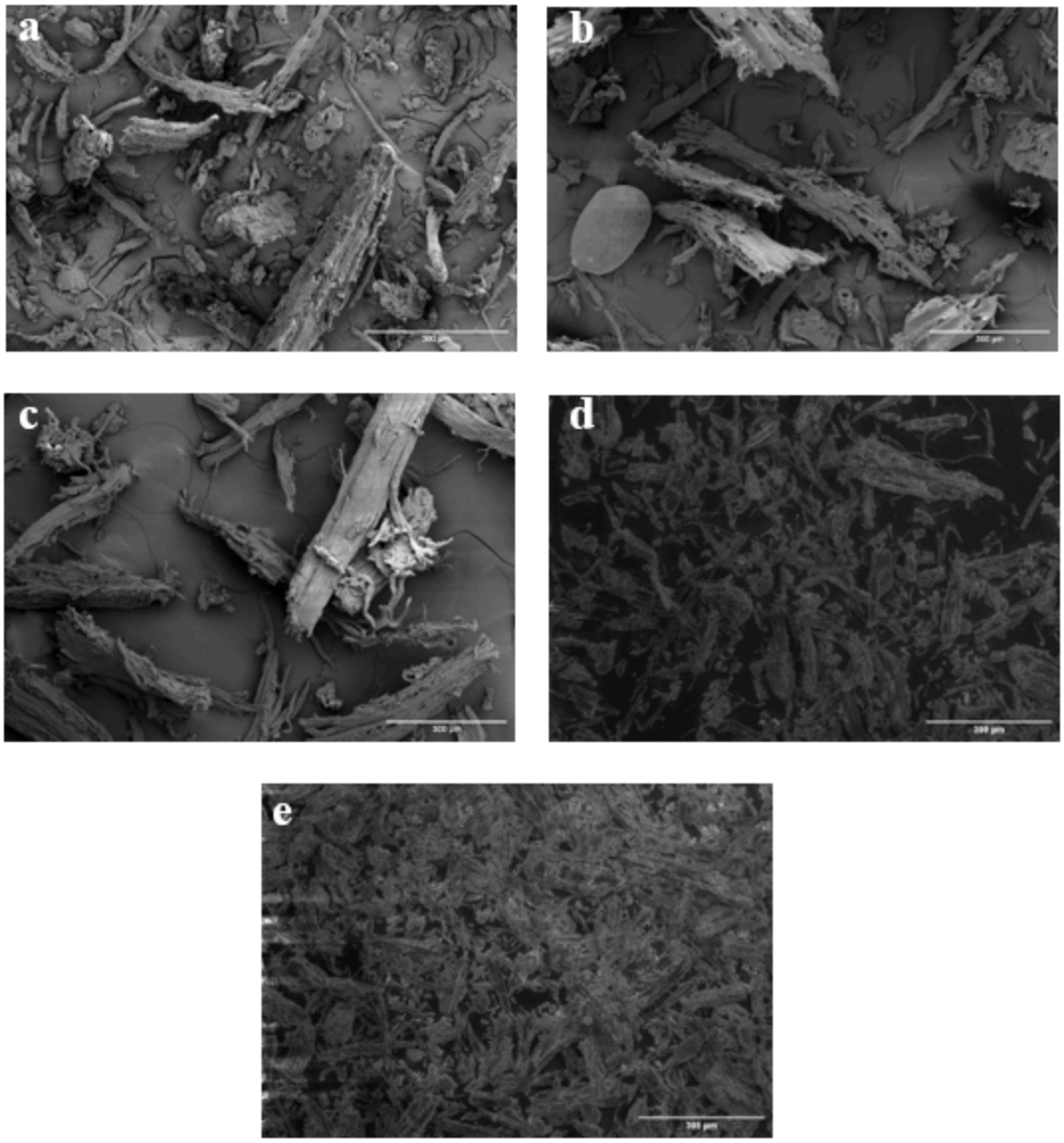

Figure 4

SEM images of raw powder (a), TPC (b), CPC (c), microwave extracted cellulose ChCl:LA (d) and ChCl:CA:H_2O (e).

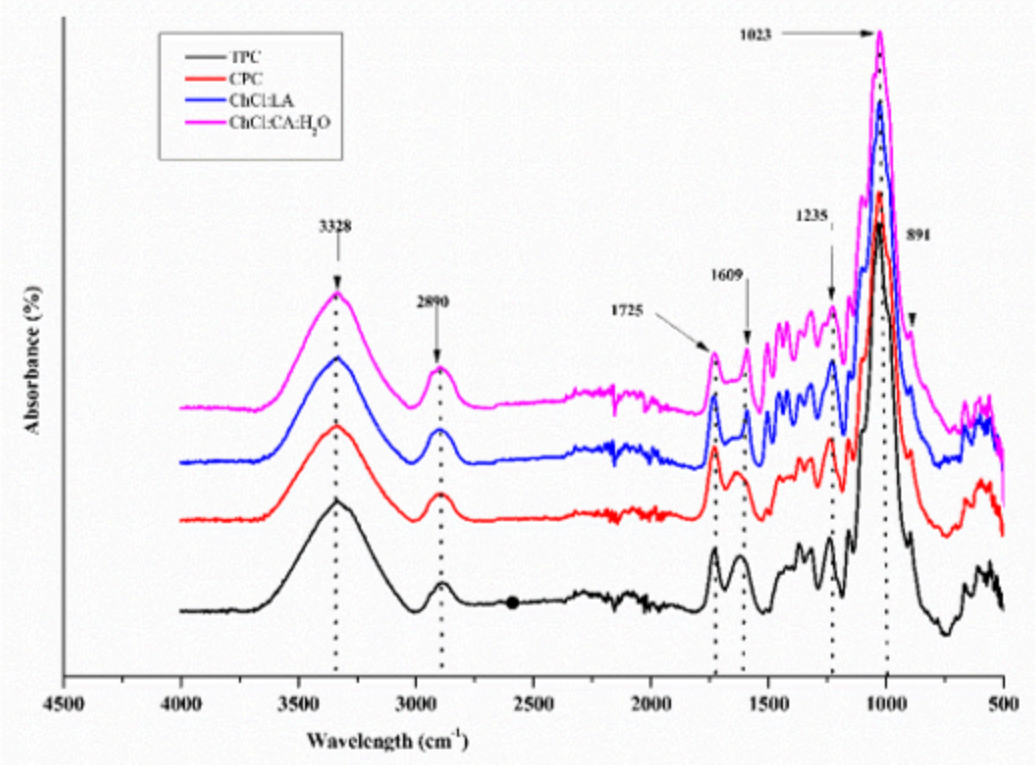

Figure 5

FT-IR spectra of TPC, CPC, ChCl:LA and ChCl:CA:H_2O samples.

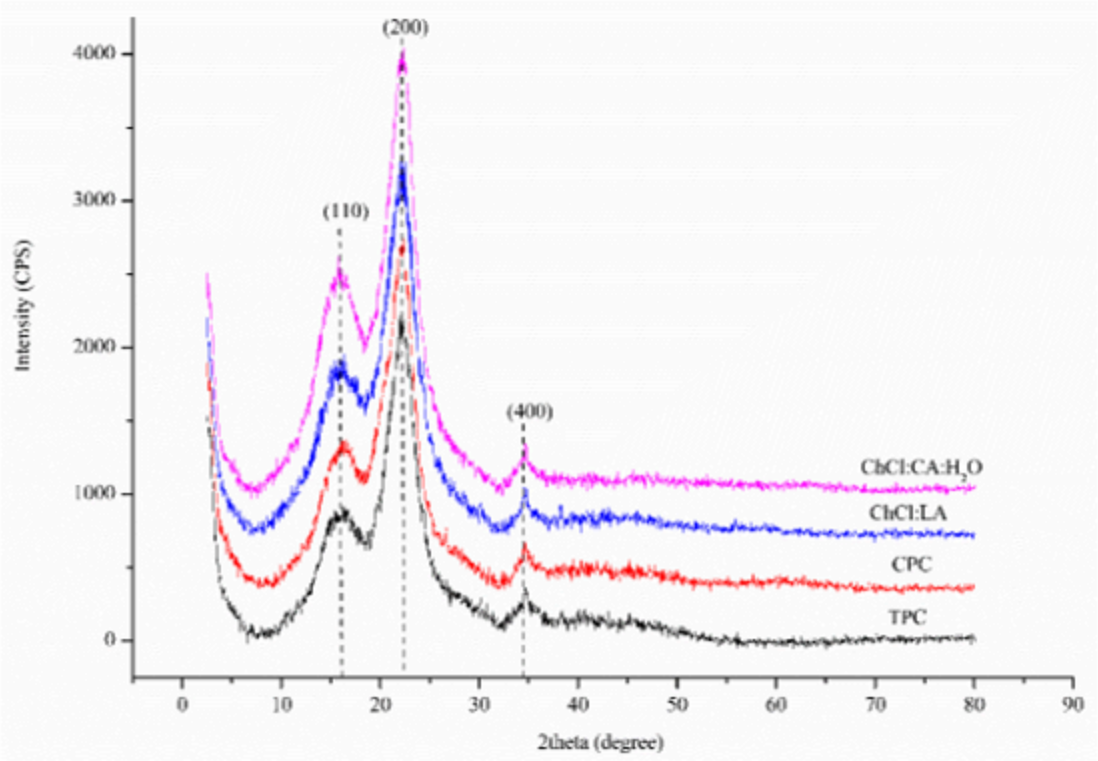

Figure 6

XRD spectra of the different cellulose materials

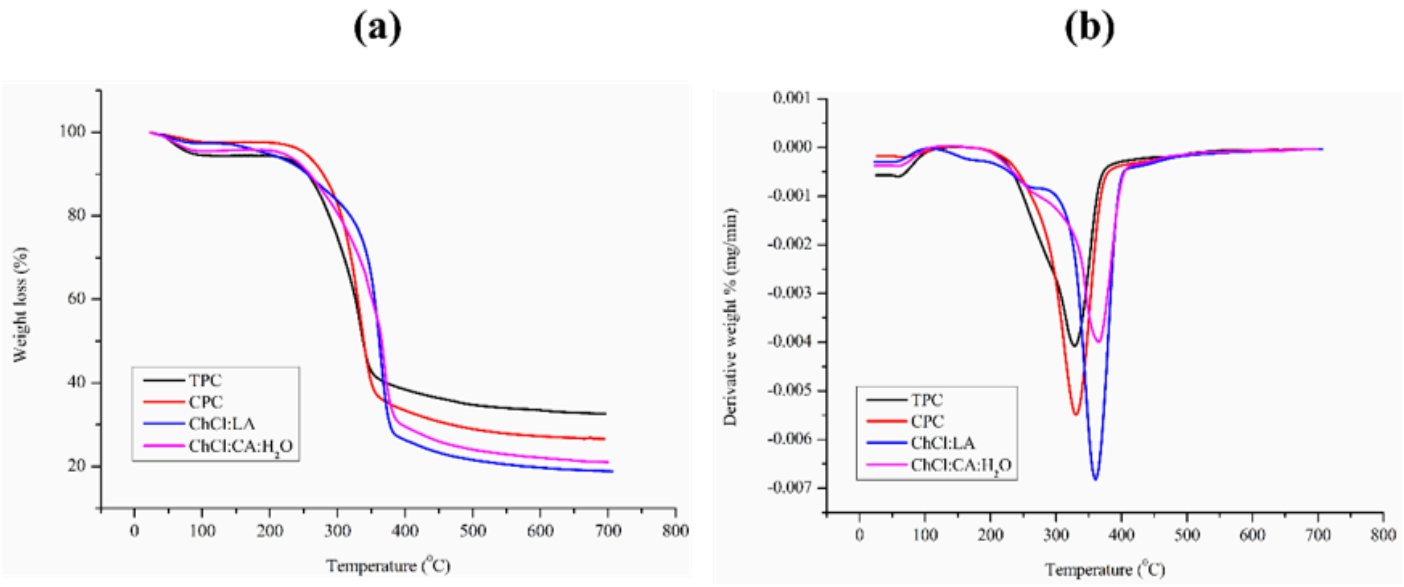

Figure 7

TGA (a) and DTG curves (b) of cellulose extracted by different processes